Supplementary materials

Navy Coastal Ocean Model (NCOM) – based results

The high-resolution operational forecasting model NCOM (Navy Coastal Ocean Model, Martin, 2000) has been widely used for the studies of the Gulf of Mexico (Poje et al., 2014; Jacobs et al., 2014; Beron-Vera et al., 2015; Ozgokmen et al., 2021). The model fields are available every 3 hours for the entire Gulf of Mexico with a horizontal resolution of 1 km. NCOM includes tides and river run off, which are two of the dominant forcing mechanisms in the northeastern GOM (the site of SPLASH experiment), and has been shown to realistically reproduce the typical ocean circulation features in the region, such as the transient, rapidly-varying submesoscale eddies of both cyclonic and anticyclonic rotation and the strong and rapidly evolving density fronts formed by the confluence of the freshwater run-off from the coast with the saltier waters from the Gulf of Mexico (Jacobs et al., 2014; Ozgokmen et al., 2021). Importantly, the model captured both the anticyclonic circulation and the two density fronts that were present in the area at the time of the SPLASH drifter experiment and that influenced the behavior of the drifters.

Because CARTHE drifters used during the SPLASH deployment were shallow and sampled the top 60 cm of the water column, we used the surface model fields to advect the simulated drifters. In order to simulate the motions of simulated drifters in the NCOM model, we used the standard variable-step 4^{th} order Runge-Kutta integration method (MATLAB's built-in function ode45) with a bi-linear velocity interpolation in time and space between the model grid points (the same integration/interpolation scheme was used in Rypina et al. (2021)).

Inspection of the model density fields (Fig. S1) suggested that the movement of SPLASH drifters was influenced by 2 density features: the dense water filament (red) that affected the northern

group of drifters during the splitting event around days 0.9-1.25, and the light water coastal plume (blue) that affected the southern group of drifters from day 1.25 and onward. Specifically, the distribution of drifters on days 1.25 through day 2 after deployment was roughly aligned with the density fronts associated with the warm and cold filaments, which formed around day 1 when the drifters were approaching the coast and which influenced the off-shore motion of the drifters during days 1.25-2. However, as is typical for numerical models, the exact location and timing of both of these features differed slightly from the real ocean circulation, as evident from the slight misalignment between the SPLASH drifters and the model fronts. (Such slight mismatch between the modeled and observed flow features is common for even the highest-resolution state-of-the-art data-assimilative oceanographic models, which tend to qualitatively reproduce the observed features but miss the small-scale details (see Rypina et al., 2021 for an example of such behavior in the Western Mediterranean Sea)). Because of these slight differences, simulated drifters released at the exact times and locations of the real drifters experienced a more northward advection during the first day after deployment and, as a result, missed the formation of the density fronts (Fig. S2a) and experienced less spreading and a weaker off-shore advection. This mismatch may be mitigated by shifting the release locations of simulated drifters about 6 km to the southeast, which allowed the simulated drifters to remain within the anticyclonic circulation during the first day and to arrive at the coast when the density fronts were still present (Fig. S2b). The simulated drifters then aligned themselves with the fronts and moved off-shore to the southwest, in a qualitative agreement with the real drifters. Because the behavior of the simulated drifters released at the shifted location was in a better qualitative agreement with real drifters, we have proceeded with this shifted drifter release in our subsequent analysis. Just like the real drifters, the simulated drifters from the shifted release initially started moving

anticyclonically around the recirculation feature, which brought them near the coast around day 1.5 (about half-day later than the real drifters). The drifters then split into a smaller northern and larger southern groups, the northern group aligned along the coast, and then the entire drifter ensemble proceeded offshore, all in qualitative agreement with real drifters. In Figs. S3-S10, we show FTLEs, L, CD, V_{en}, $LAVD$, D, and spectral clusters computed using segments of simulated trajectories from $t_{start} = 0$ days to $t_{end} = 0.5$, 2 and 4 days, respectively. These are the simulated-drifter-based counterparts of Figs. 3-9. Then we re-computed the same quantities using dense regularly-spaced orthogonal grids of simulated drifters in order to investigate possible biases arising due to the limited number of SPLASH drifters and the non-regularity/non-orthogonality of the SPLASH release grid. In the remainder of the paper we will refer to the model fields computed using simulated SPLASH-like drifters as the "SPLASH-like" simulations, and to the model fields computed using the dense regular orthogonal grids as the "true" model fields.

FTLEs (Fig. S3): At the initial stage of motion ($t_{end} = 0.5$ days), the SPLASH-like FTLEs showed a zonal swath of larger values (where the drifters diverged more strongly) extending from the western corner of the release domain, with smaller FTLEs to the north and south of it. There was also a small region of negative FTLEs in the north, where drifters converged closer together, instead of separating from each other. These features bore some degree of qualitative and quantitative similarity to the real-drifter FTLEs in Fig. 4, in that the patterns of high and low values were somewhat similar and the magnitudes of variation were the same. Comparison with the true model FTLEs (second row) showed excellent agreement, as both the zonal swath of the large FTLEs extending from the west and the negative-FTLE region in the north were clearly present, and the magnitudes of FTLEs were also comparable between the two cases.

At the intermediate stage of motion ($t_{end} = 2$ days) when the simulated drifters approached the coast, split to the north/south and formed an elongated along-shore filament, the SPLASH-like FTLEs looked more complex than at the initial stage, but several features could still be easily teased out. In the western half of the release domain, a zonal filament of larger FTLE values (similar to the one at 0.5 days) extending from the western corner was still visible, with smaller values to the north and south from it. In the eastern half of the domain, the FTLE structures were less clear, with intermingled small clusters of high and low FTLEs located next to each other. True model FTLEs revealed the presence of several maximizing ridges within the domain – the elongated filament extending from the west at about 29.025N (that was also present at 0.5 days), the S-shaped ridge entering the domain from the east at about 29.07N, and a strong ridge in the south extending across the entire domain (plus some other shorter and weaker ridges in other parts of the domain). Because the distances between these individual ridges were in some cases comparable to the spacing between SPLASH drifters, these features were under-resolved by the SPLASH-like release and, as a result, led to a noisier FTLE map. Despite this complication, the agreement between the SPLASH-like and the true model FTLEs was still favorable.

Finally, during the third stage of motion ($t_{end} = 4$ days), when the drifters went further offshore, SPLASH-like FTLEs showed a very clear distinction between the high values along the southeastern edge of the domain and smaller values elsewhere. There was also a small cluster of slightly elevated FTLEs in the northwest around 89.575W, 29.05N, as well as a few clusters of slightly negative FTLEs scattered around the domain. Comparison with the true model FTLEs revealed that the FTLE field was dominated by 2 strongest ridges – the S-shaped ridge in the east and the very strong nearly-zonal ridge in the south. Neither of these ridges was well resolved by the SPLASH drifters, but the red cluster in the 5th row of Fig. 12 seemed to contain trajectories

92 located to the east from the S-shaped ridge. Note also that several small regions of slightly
93 negative values present in the SPLASH-like FTLE maps agree well with the true model fields.
94 Overall, because of the smaller number of distinctive features present within the domain,
95 SPLASH-like FTLE maps at 4 days were even cleaner and easier to interpret than those at 2
96 days, and they agreed very well with the true model FTLEs.
97
98 *L* and *CD (Figs. S4-S5):* Being measures of complexity of individual trajectories (rather than
99 measures involving groups of trajectories), both *L* and *CD* do not depend on the release grid.
100 Despite this advantage, SPLASH-like *L*-and *CD*-maps were still only marginally useful in
101 identifying the dominant LCSs. Similar to the real-drifters, SPLASH-like *L* and *CD* fields at all
102 times were dominated by a large-scale gradient, with smaller values in the north (or northeast
103 during the initial stage of motion) and larger values in the south (or southwest at for the initial
104 stage). All other features, which in the true model maps showed up as the sharp smaller-scale
105 gradients embedded into the above-mentioned large-scale gradient, were not resolved by the 135
106 SPASH-like simulated drifters.
107
108 V_{en} *(Fig. S6):* Encounter volume at early times was not particularly informative. SPLASH-like
109 V_{en} in the top panel did not show any distinguishing features, and the true model fields were
110 uniform over most of the domain. This is because the drifters did not have time to encounter
111 many of their neighbors. At intermediate stage of motion ($t_{end} = 2$ days), the V_{en} fields
112 developed significantly more. Specifically, going from south to north, SPLASH-like map
113 showed very small values in the south, a region containing higher values (or perhaps 2 separate
114 maximizing ridges) further north of it, with the values diminishing again to the north. All of

these features agreed well with the true model fields, which indeed showed smallest encounter volume in the south, then 2 separate maximizing ridges in the middle part of the domain, with blue value further north. At the third stage of motion ($t_{end} = 4$ days), the dominant features were similar, with additional several maximizing ridges complicating the picture. Agreement between the SPLASH-like and the true model maps was again quite good, but distinguishing all the various individual ridges within the SPLASH-like maps became increasingly challenging with time. It is interesting to note that at 4 days the true model field showed quite a bit or red in the bottom left panel but seemed mostly blue in the bottom middle and right panels. This is because trajectories released in the southern (blue V_{en}) part of the release domain experienced fast separations and formed a long blue tail that visually dominated the distribution, with most non-blue values confined to the smaller area near 90W and 28.82N. Overall, encounter volume worked best at intermediate times when the drifters had enough time to encounter their neighbors but when the dominant LCSs were not overly complex to be resolved by the 135 SPLASH-like drifters.

D (Fig. S7): Dilation at the initial stage of motion ($t_{end} = 0.5$ days), showed a zonal stripe of larger positive values extending into the domain from the west, with smaller values to the north and south. In the very south of the domain, the values increased again. In the north, dilation decreased and became negative in the northern corner. Both the zonal stripe and the convergence region in the north agreed with their counterparts identified using FTLE maps. True model dilation, computed by integrating the Eulerian model divergence along trajectories released on a dense grid, was in excellent agreement with the SPLASH-like *D* maps. At longer times, the agreement between SPLASH-like and true model maps was still good when and where dilation

could be reliably computed, but because many drifters separated from their neighbors too far and/or aligned into polygons that were overly elongated, SPLASH-like dilation fields became gappy. Overall, dilation seemed a useful diagnostic when/where it can be reliably computed, but its estimation from limited drifter data became increasingly challenging with time due to the separation and alignment of the drifters.

LAVD (Fig. S8): At early times, $LAVD$ was dominated by the large values in the south, which were clearly visible in both SPLASH-like and true model maps. There was also a stripe of slightly elevated values entering from the western corner of the domain, which was reminiscent of the features observed in the FTLE maps. At longer times, $LAVD$ became increasingly gappy and noisy, but where/when it could be reliably computed, it still agreed well with the true model values (computed by integrating Eulerian model estimates along trajectories). The main features at the intermediate and later stages were the blue cluster at 89.525W, 29.3N, the red filament entering the domain from the western corner, a red clusters in the very south, and another red cluster near the southeastern edge of the domain (which coincided with the area to the east of the letter-S-shaped filament identified in the FTLE maps). Most of these features could only be resolved in the dense true model maps but not SPLASH-like maps. Overall, SPLASH-like $LAVD$ maps were reliable, as suggested by the good agreement with their true model counterparts, and were able to map out some of the dominant flow features, even though SPLASH-like maps did not fully resolve them.

SC (Fig. S9-S10): For the simulated SPLASH-like drifters (Fig. S9), the optimized parameter spectral clustering identified 2 cluster configurations for each time. (We remind the reader that

the optimized parameter spectral clustering algorithm sweeps through a range of values for the sparsification radius – the parameter defining the size of the resulting spectral clusters – to find optimal values that correspond to the local maxima in normalized eigengap.) At the initial stage of motion, both optimal cluster configurations consisted of 14 different clusters, which is similar to the number of spectral clusters for the real drifters at early times. Also, just like in the case with real drifters, the number of clusters for simulated SPLASH-like drifters decreased with time. At the intermediate stage of motion, again 2 optimal cluster configurations were identified – one with 9 and another with 6 clusters. In both cases, the release domain was split zonally at about 29N into a larger northern and a smaller southern cluster, with a few trajectories in the very south of the release domain assigned to their own separate clusters. When mapped to the current position of the drifters, those southern trajectories lined up along the tail part of the distribution extending to the west. In the case with 9 clusters, the large northern cluster was additionally split into two. At the third stage of motion, there were again 2 optimal cluster configurations –with 6 and 4 clusters. For the former, most of the domain was assigned to one blue cluster, with the second smaller yellow cluster containing trajectories in the east, and three very small clusters in the very south of the release domain. When mapped to the current drifter positions, the splitting pattern became more obvious, with the body of the distribution assigned to one main blue cluster, and with the yellow cluster containing southern trajectories; 2 trajectories in the very north were assigned to their own clusters. For the configuration with 4 clusters, the release domain was split into 2 large clusters – blue and orange, with 2 trajectories in the south assigned to their own separate clusters.

For the true model spectral clusters (Fig. S10), the method also identified several optimal delineations of the domain into clusters at each time. For the early stage, all configurations had a

large number of clusters (between 9 and 19), similar to the SPLASH-like spectral clustering results. In Fig. S10, we show an optimal division of the domain with the minimum (9) and maximum (19) number of clusters. At the intermediate stage of motion, there were two optimal configurations, one with 18 and another with 16 clusters. However, unlike at earlier times, many clusters were small and located on the periphery of the domain, outside of the SPLASH-like release domain in Fig S9. Thus, despite the overall large number of clusters identified at the intermediate stage of motion, the number of clusters within the SPLASH domain was significantly smaller than at the early stage, which agrees well with the SPLASH-like results. In particular, the configuration with 16 clusters assigned the entire SPLASH domain to one blue cluster, whereas the configuration with 18 clusters divided the SPLASH domain into two clusters, with the division curve at near 29N, similar to the results for the SPLASH-like simulated drifters in Fig. S9. The situation with 4 days is in many aspects similar to that at 2 days. Specifically, the optimized parameter spectral clustering identified several optimal configurations with a large number of clusters, from 7 to 17. However, in all of these configurations, a large number of small clusters were located near the southern edge of the domain, outside of the SPLASH domain in Fig. S9, with the bulk of the SPLASH domain assigned to just one cluster (a representative spectral cluster configuration at 4 days is shown in the bottom row of Fig. S10). Overall, the spectral clusters in Fig. S10 were similar to those in Fig. S9 in regions where the two domains overlapped, thus suggesting that the spectral clusters identified using SPLASH-like drifters were similar to the true spectral clusters in the model.

In additional simulations (not shown), we have also investigated the robustness of all dynamical systems quantities to the GPS positioning noise in the drifter data by adding a random displacement (taken from a normal distribution with STD of 5 m) to the simulated drifter

trajectories in the NCOM model. Not surprisingly, such noise has a negligible effect on FTLEs, N_{en}, and Spectral Clusters (because 5 m is negligible compared to the distances between the drifters), has a weak effect on L and CD (because these are integral quantities of the subsequent drifter position differences), and a stronger effect on D and $LAVD$ (both because these are integral quantities and because the position disturbance of 5 m may be significant for the estimation of the local derivatives of velocity). When working with noisy data, applying a smoothing filter (for example, a running average) to the drifter trajectories, as was done in Rypina et al. (2021), may suppress noise, reduce errors in divergence and vorticity, and improve D and $LAVD$ estimates.

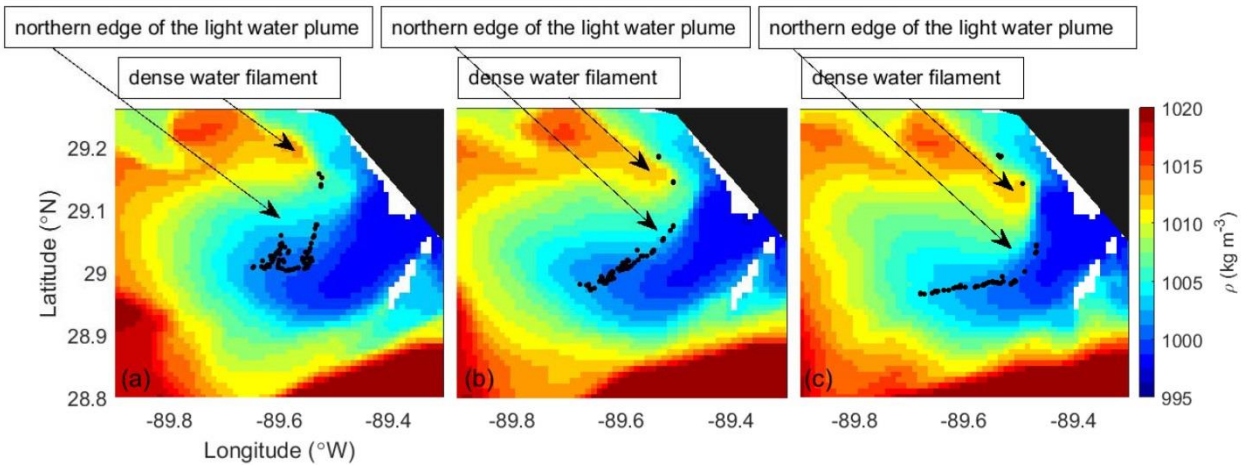

Figure S1. SPLASH drifter positions superimposed on the model surface density fields on days (a) 1; (b) 1.25; and (c) 1.5 after the release.

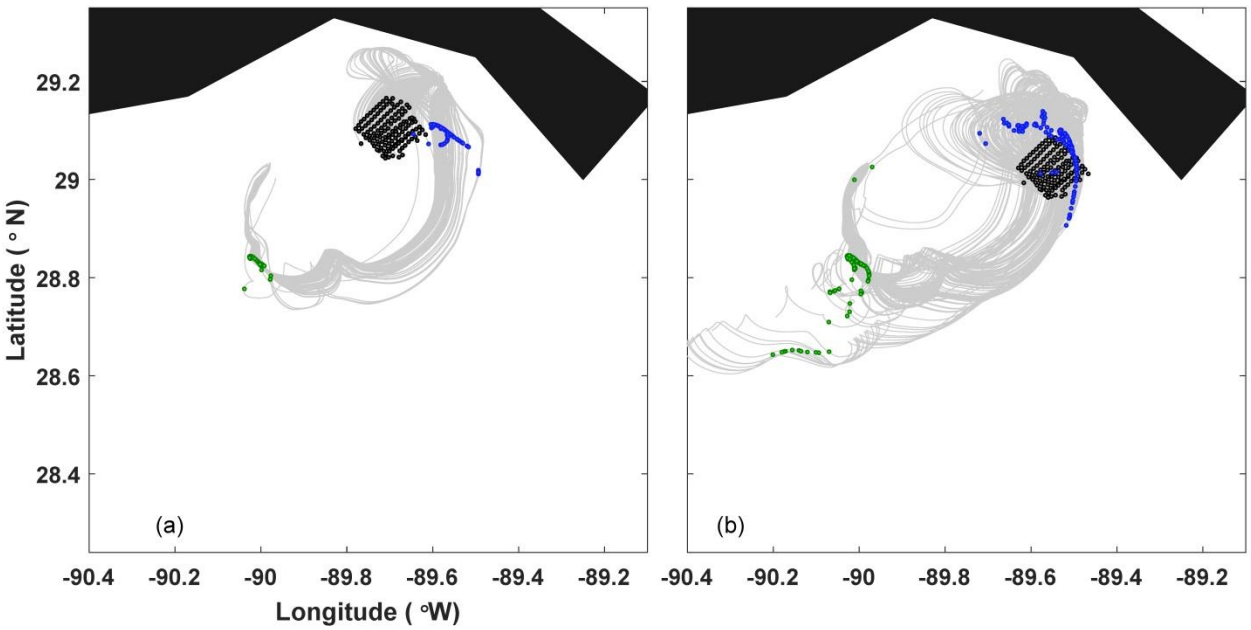

Figure S2. (a) Trajectories of the NCOM-simulated drifters released at the times and locations of the real SPLASH drifters, with the positions at the release time, 2 days, and 4 days shown by black, blue and green dots, respectively. Trajectories of the NCOM-simulated drifters released at the slightly shifted locations, with the positions at the release time, 2 days, and 4 days shown by black, green and blue dots.

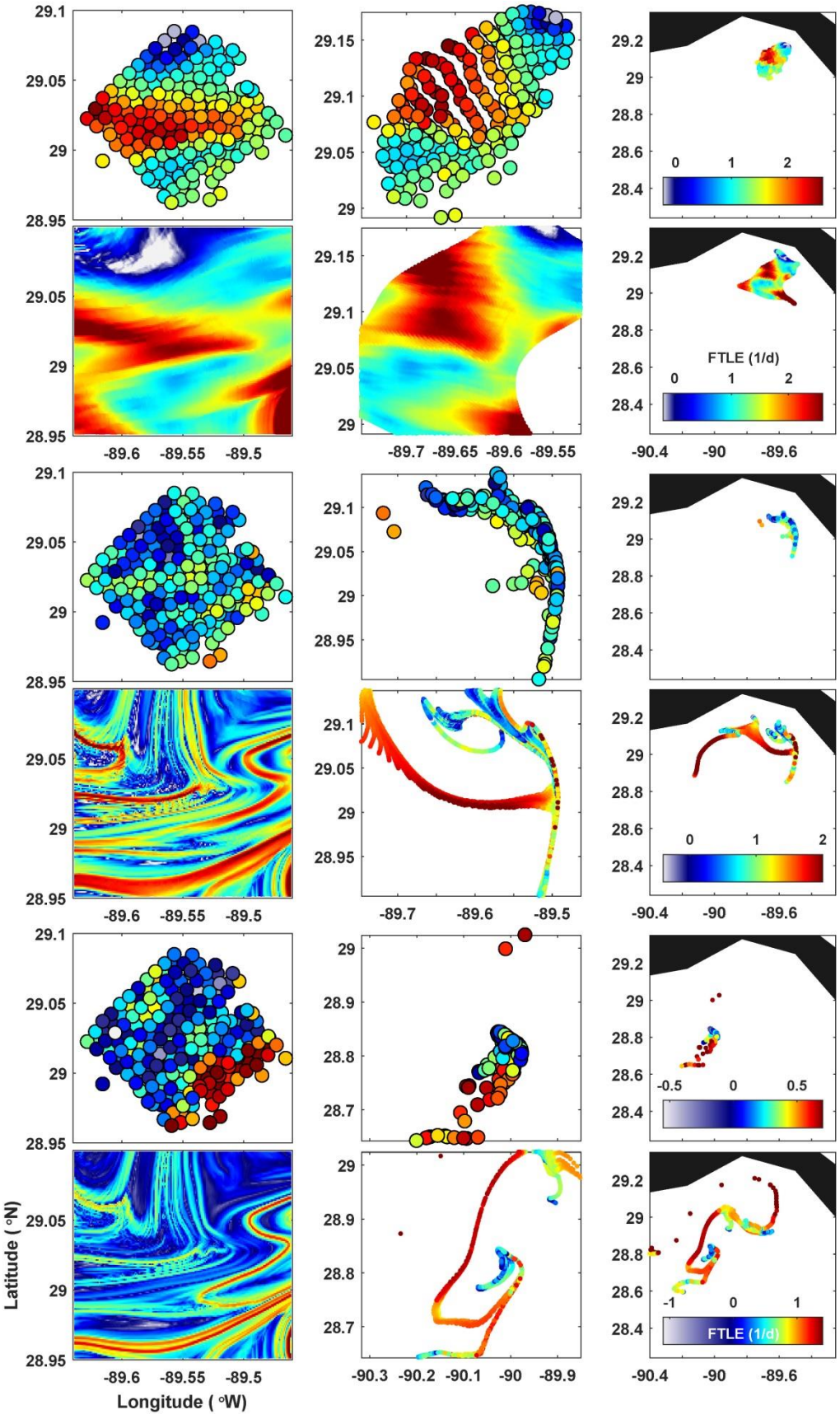

244

245

246

Figure S3. Model-based FTLEs at 0.5 (rows 1-2), 2 (rows 3-4) and 4 (rows 5-6) days for simulated SPLASH drifters (rows 1,3,5) and for drifters released on a dense regular orthogonal grid (rows 2,4,6). Fields are mapped to the initial (left) and current (middle and right) positions of the simulated drifters.

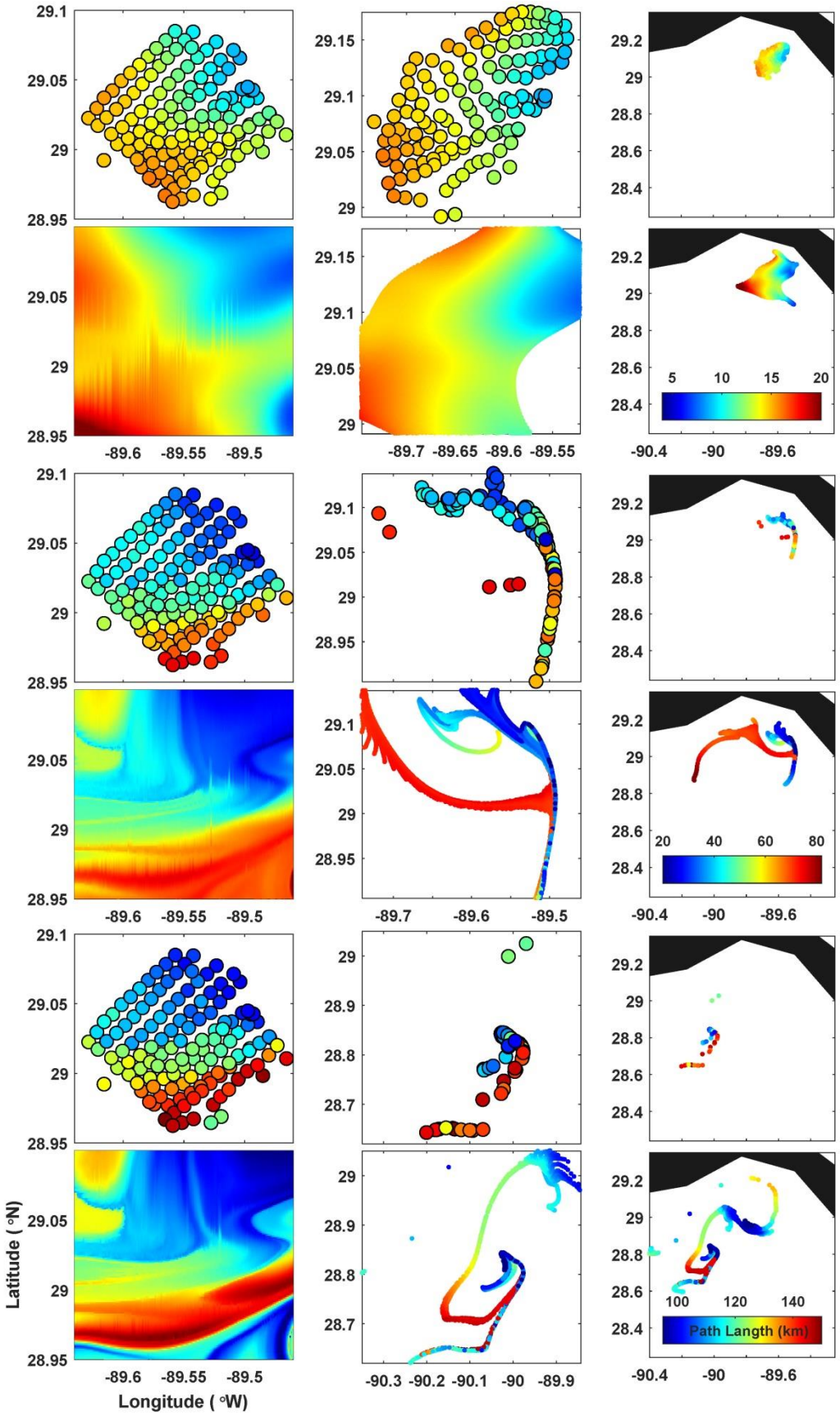

257

258

259

Figure S4. Model-based path length at 0.5 (rows 1-2), 2 (rows 3-4) and 4 (rows 5-6) days for simulated SPLASH drifters (rows 1,3,5) and for drifters released on a dense regular orthogonal grid (rows 2,4,6). Fields are mapped to the initial (left) and current (middle and right) positions of the simulated drifters.

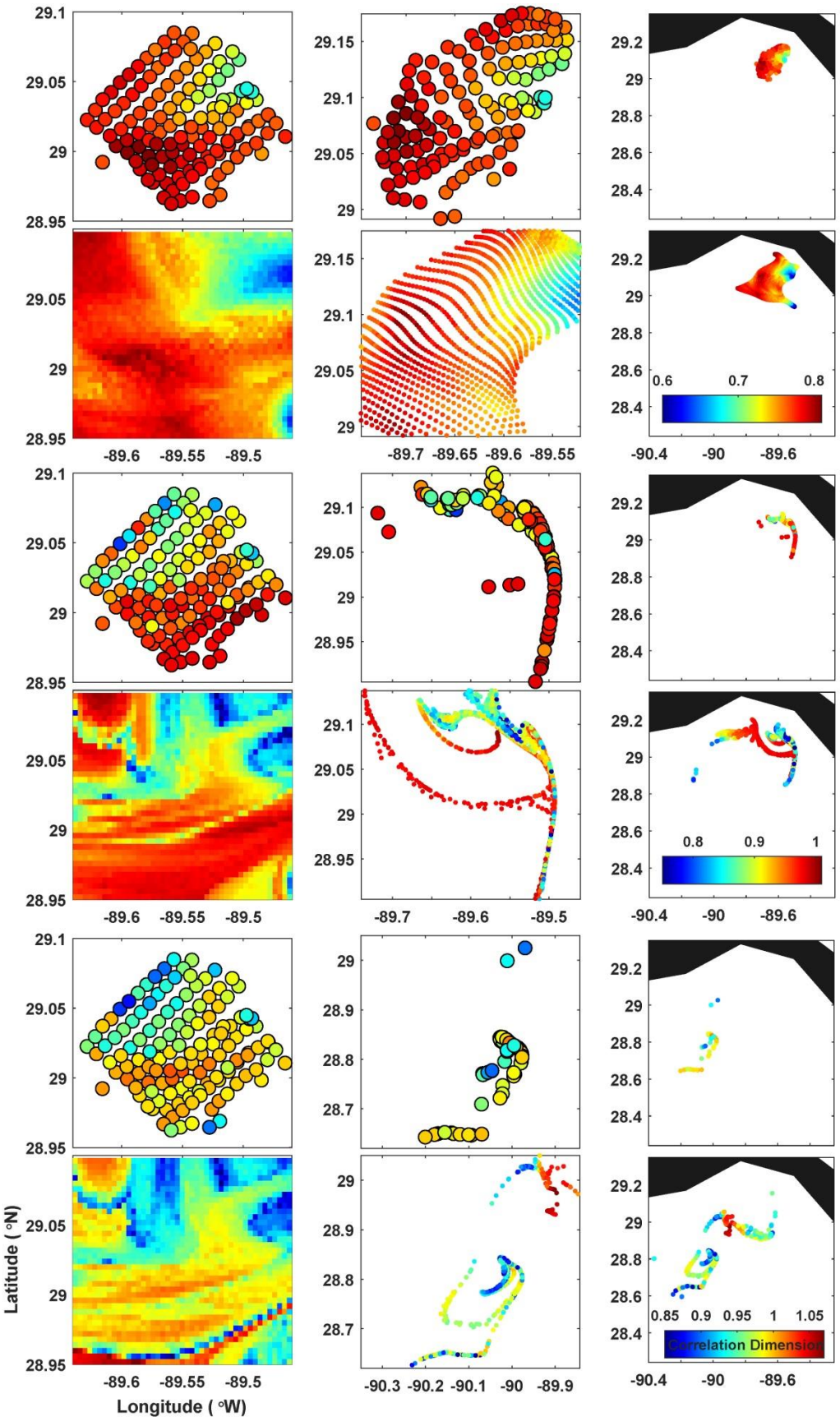
Latitude (°N)
Longitude (°W)
Correlation Dimension

Figure S5. Model-based correlation dimension at 0.5 (rows 1-2), 2 (rows 3-4) and 4 (rows 5-6) days for simulated SPLASH drifters (rows 1,3,5) and for drifters released on a dense regular orthogonal grid (rows 2,4,6). Fields are mapped to the initial (left) and current (middle and right) positions of the simulated drifters.

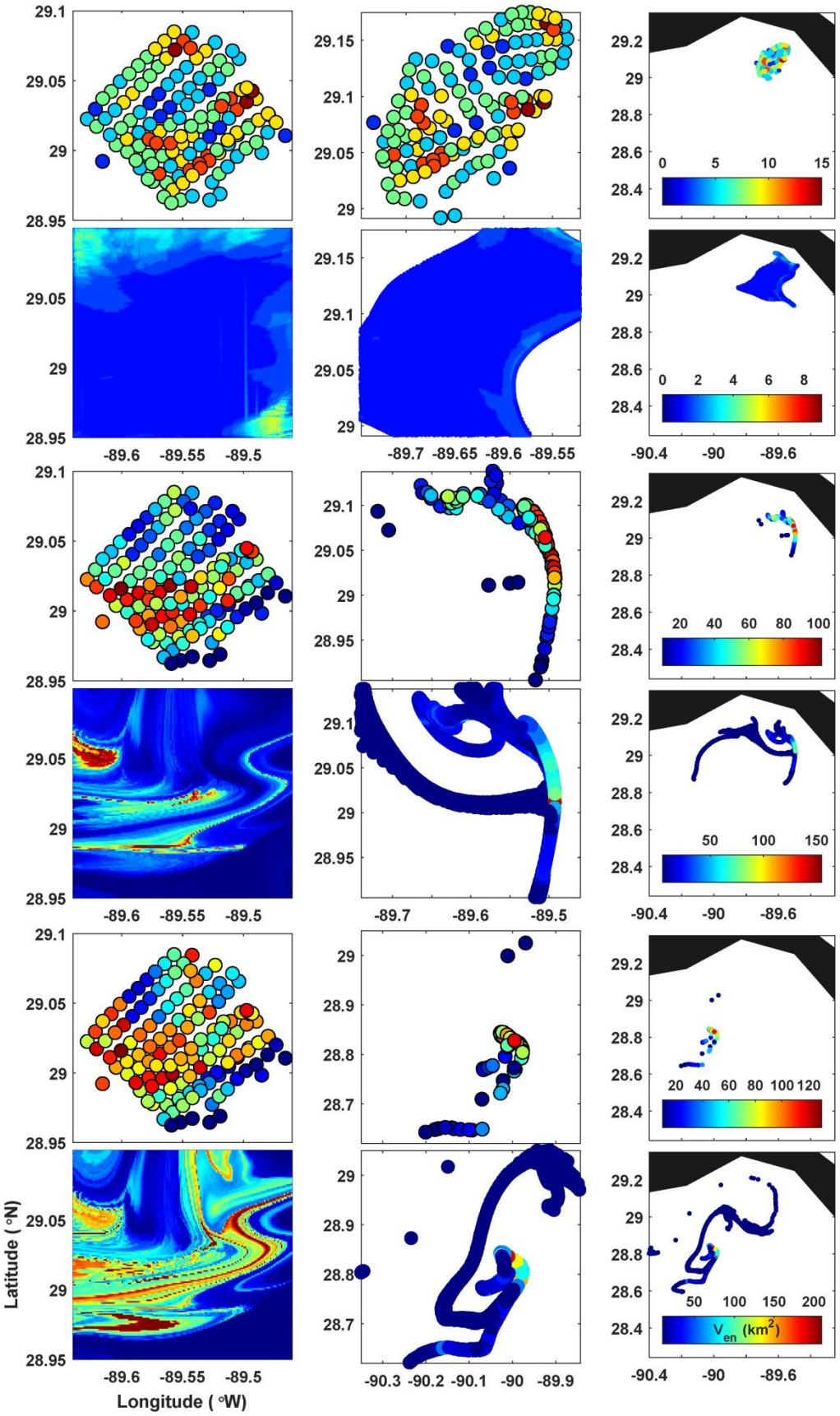

285

286

287

Figure S6. Model-based encounter volume at 0.5 (rows 1-2), 2 (rows 3-4) and 4 (rows 5-6) days for simulated SPLASH drifters (rows 1,3,5) and for drifters released on a dense regular orthogonal grid (rows 2,4,6). Fields are mapped to the initial (left) and current (middle and right) positions of the simulated drifters.

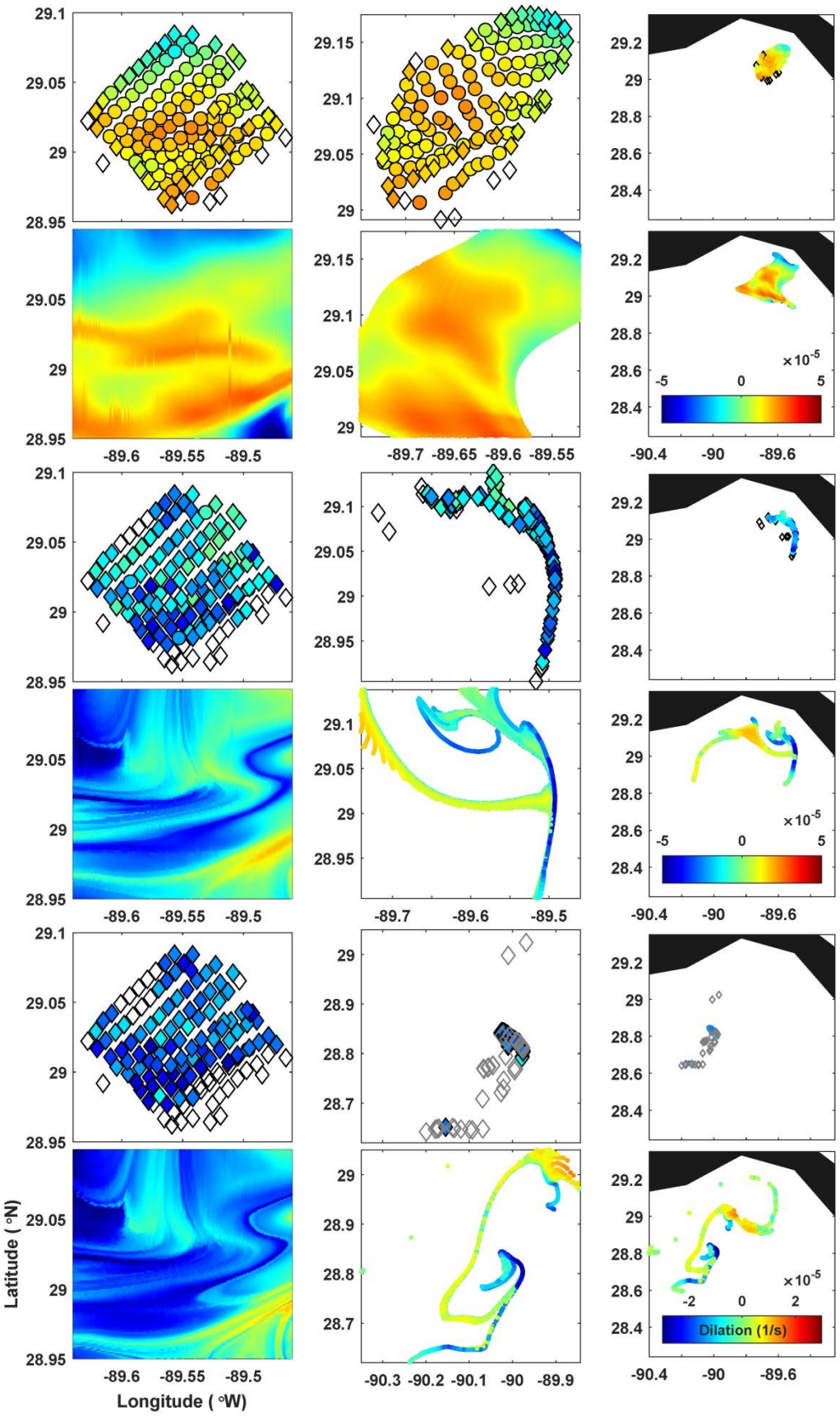

307

308

309

Figure S7. Model-based dilation at 0.5 (rows 1-2), 2 (rows 3-4) and 4 (rows 5-6) days for simulated SPLASH drifters (rows 1,3,5) and for drifters released on a dense regular orthogonal grid (rows 2,4,6). Fields are mapped to the initial (left) and current (middle and right) positions of the simulated drifters.

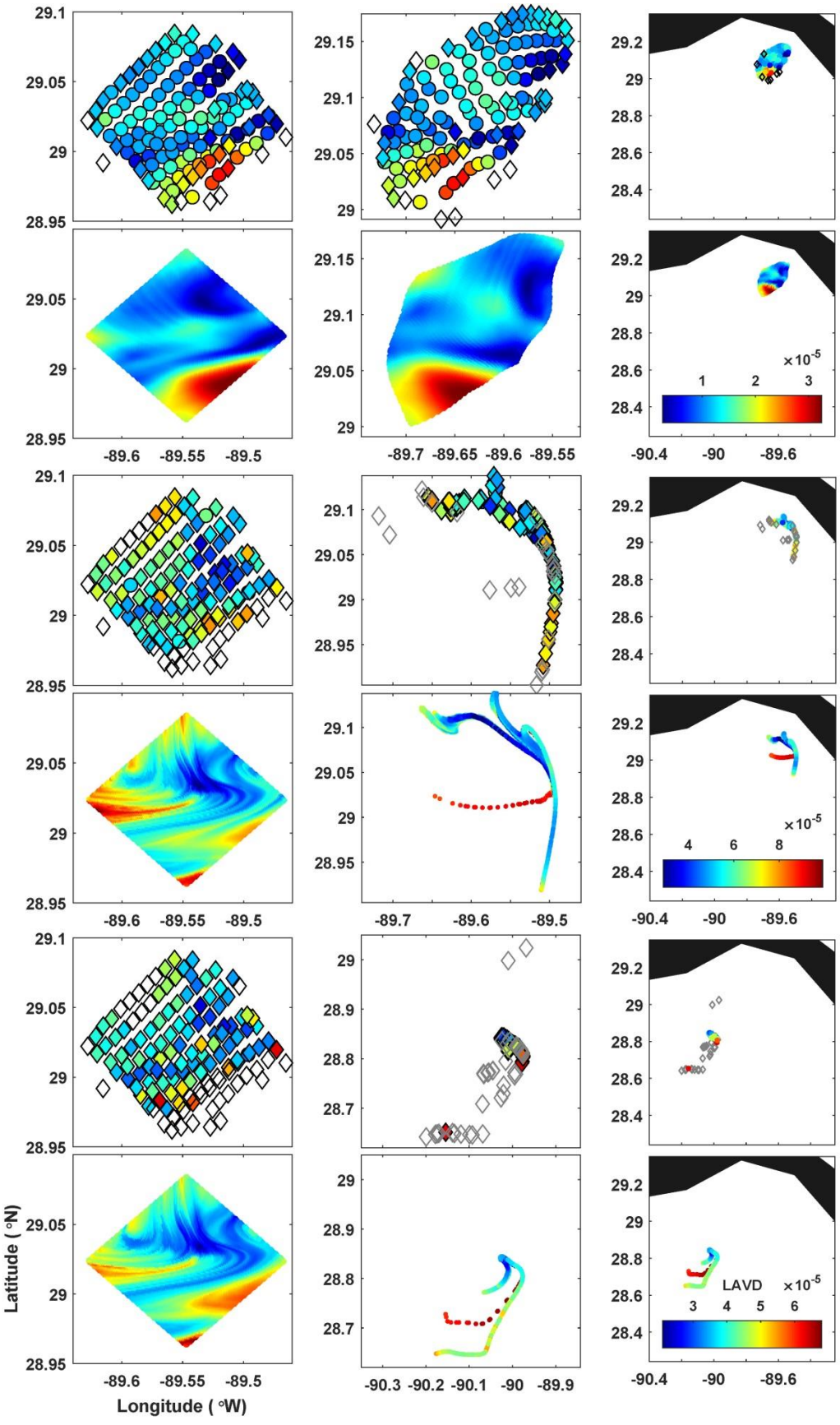
Latitude (°N)
Longitude (°W)
LAVD
×10^-5
1 2 3
4 6 8
3 4 5 6

Figure S8. Model-based LAVD correlation dimension at 0.5 (rows 1-2), 2 (rows 3-4) and 4 (rows 5-6) days for simulated SPLASH drifters (rows 1,3,5) and for drifters released on a dense regular orthogonal grid (rows 2,4,6). Fields are mapped to the initial (left) and current (middle and right) positions of the simulated drifters.

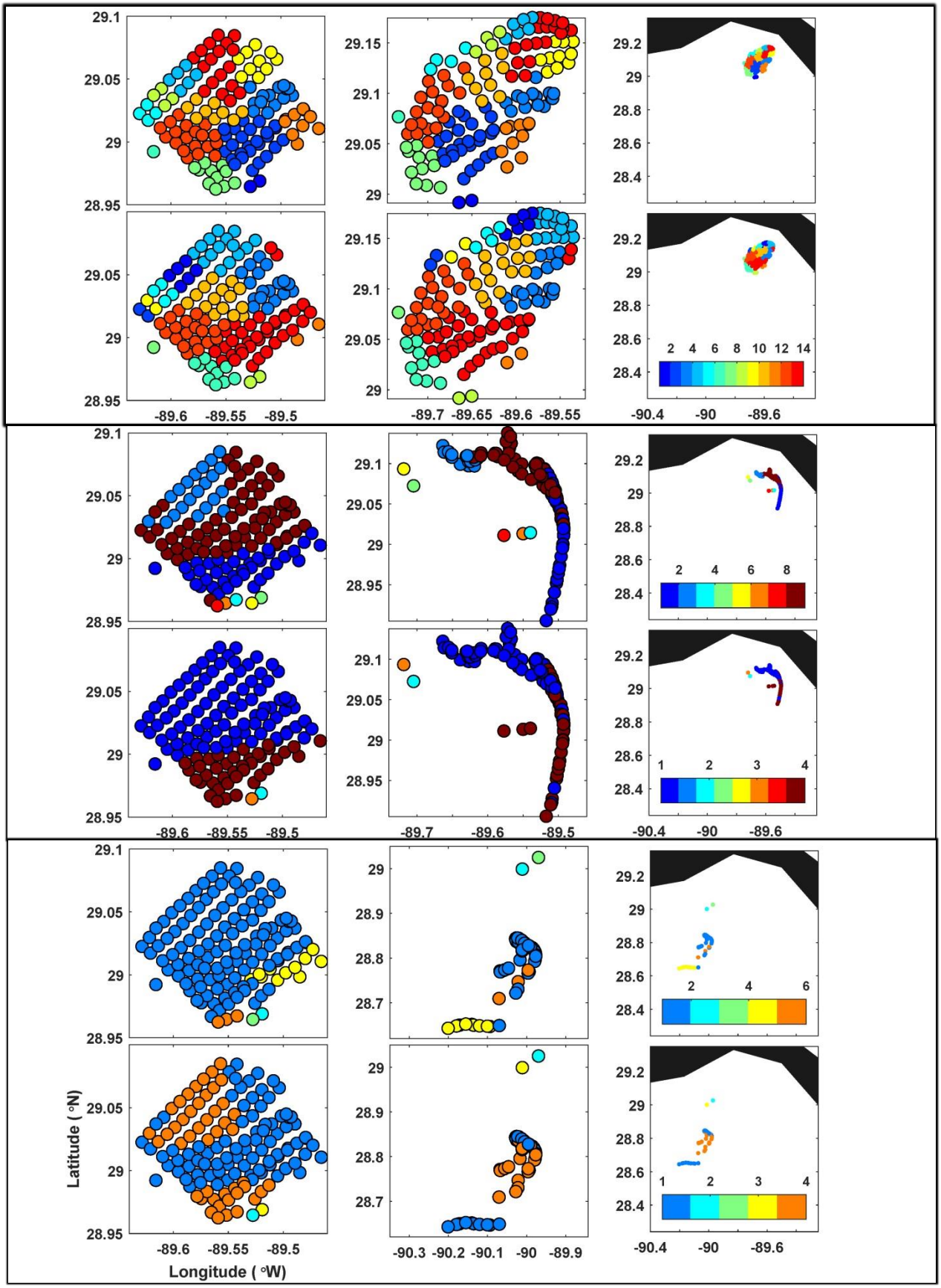
29.1
29.05
29
28.95
-89.6 -89.55 -89.5
29.15
29.1
29.05
29
-89.7 -89.65 -89.6 -89.55
29.2
29
28.8
28.6
28.4
2 4 6 8 10 12 14
-90.4 -90 -89.6
2 4 6 8
1 2 3 4
28.9
28.7
2 4 6
-90.3 -90.2 -90.1 -90 -89.9
Latitude (°N)
Longitude (°W)

351

Figure S9. Spectral clusters for simulated SPLASH drifters at T=0.5 days (rows 1-2); T=2 days (rows 3-4); and T=4 days (rows 5-6). Fields are mapped to the initial (left) and current (middle and right) positions of the simulated drifters.

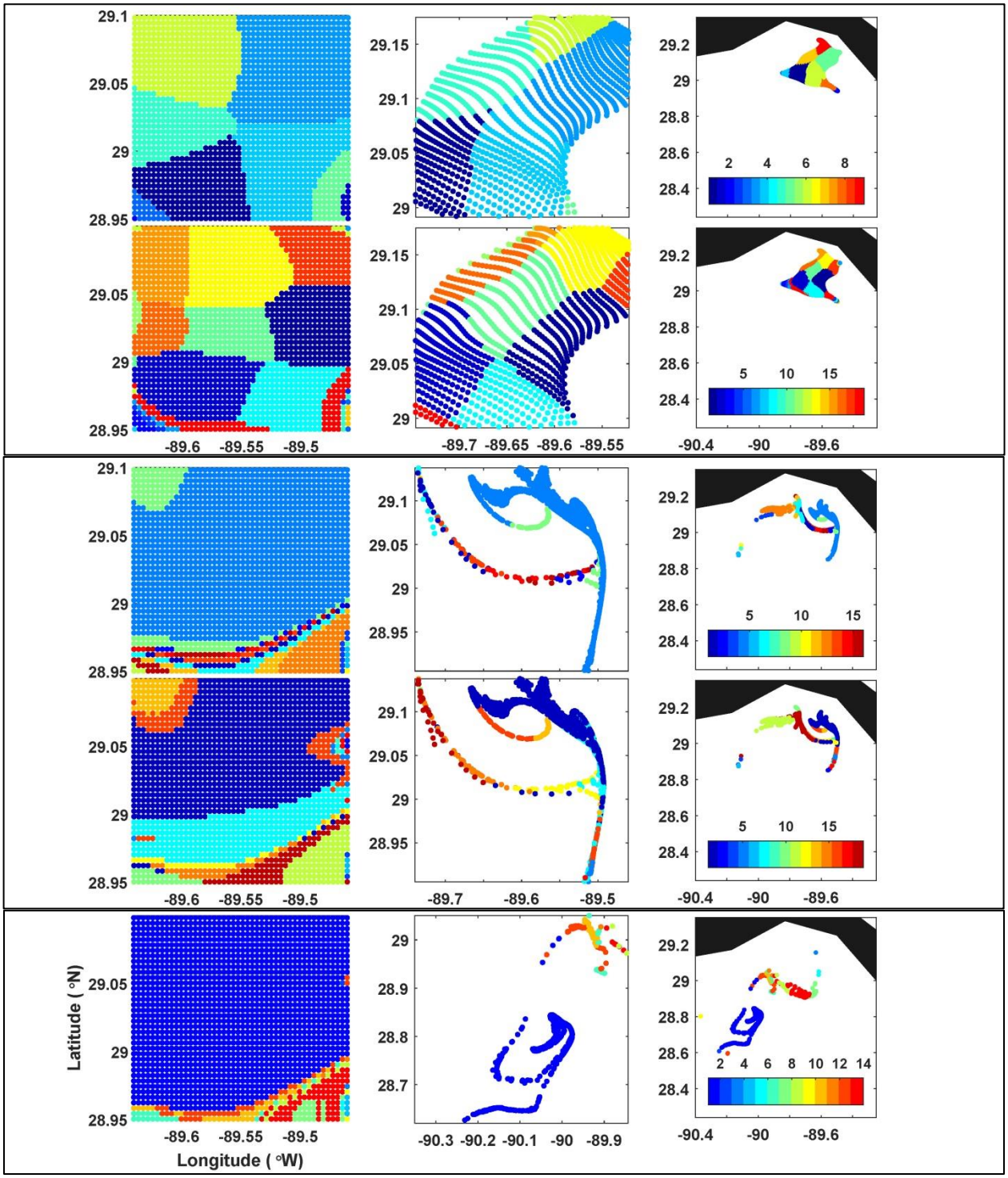

Figure S10. True model spectral clusters computed using simulated trajectories released on a dense regular grid at T=0.5 (rows 1-2); 2 days (rows 3-4); and 4 days (row 5). Fields are mapped to the initial (left) and current (middle and right) positions of the simulated drifters.

355